

Hybrid Theory-Based Time-Optimal Control of an Electronic Throttle

Mario Vašak, Mato Baotić, *Member, IEEE*, Ivan Petrović, *Member, IEEE*, and Nedjeljko Perić, *Senior Member, IEEE*

Abstract—An electronic throttle is a dc-motor-driven valve that regulates air inflow into the combustion system of the engine. The throttle control system should ensure fast and accurate reference tracking of the valve plate angle while preventing excessive wear of the throttle components by constraining physical variables to their normal-operation domains. These high-quality control demands are hard to accomplish since the plant is burdened with strong nonlinear effects of friction and limp-home nonlinearity. In this paper, the controller synthesis is performed in discrete time by solving a constrained time-optimal control problem for the piecewise affine (PWA) model of the throttle. To that end, a procedure is proposed to model friction in a discrete-time PWA form that is suitable both for simulation and controller design purposes. The control action computation can, in general, be restated as a mixed-integer program. However, due to the small sampling time, solving such a program online (in a receding horizon fashion) would be very prohibitive. This issue is resolved by applying recent theoretical results that enable offline precomputation of the state-feedback optimal control law in the form of a lookup table. The technique employs invariant set computation and reachability analysis. The experimental results on a real electronic throttle are reported and compared with a tuned PID controller that comprises a feedforward compensation of the process nonlinearities. The designed time-optimal controller achieves considerably faster transient, while preserving other important performance measures, like the absence of overshoot and static accuracy within the measurement resolution.

Index Terms—Constrained systems, constrained time-optimal control (CTOC), control invariant set, discrete-time (DT), dynamic programming, electronic throttle, friction, limp-home (LH) nonlinearity, piecewise affine (PWA) systems.

I. INTRODUCTION

MANY of the vital functions of today's cars are shifting from a purely mechanical to an electromechanical implementation. These so-called "X-by-wire" systems [1], [2] act as an interface between the driver and the targeted mechanical subsystem of the vehicle (e.g., brakes, throttle valve). Coupled with the use of advanced control strategies the "X-by-wire" systems can, in general, provide wider functionality and better

Manuscript received January 18, 2006; revised November 29, 2006. Abstract published on the Internet January 27, 2007. This work was supported in part by the Ministry of Science, Education and Sports of the Republic of Croatia and in part by the Swiss National Science Foundation.

M. Vašak, I. Petrović, and N. Perić are with the Faculty of Electrical Engineering and Computing, University of Zagreb, 10000 Zagreb, Croatia (e-mail: mario.vasak@fer.hr).

M. Baotić is with the Faculty of Electrical Engineering and Computing, University of Zagreb, 10000 Zagreb, Croatia, and also with the Automatic Control Laboratory, Swiss Federal Institute of Technology, 8092 Zurich, Switzerland.

Color versions of one or more of the figures in this paper are available online at <http://ieeexplore.ieee.org>.

Digital Object Identifier 10.1109/TIE.2007.893060

efficiency of the vehicle. In this paper, we focus on the throttle-by-wire system.

The electronic throttle is essentially a dc-motor-driven valve that regulates air inflow into the vehicle's combustion system. The electronic throttle control (ETC) system positions the throttle valve according to the reference opening angle provided by the engine control unit (ECU). Today's ECUs use lookup tables with several thousands entries [2] to find the fuel and air combination which maximizes fuel efficiency and minimizes emissions while respecting drivers intentions (i.e., the gas pedal position). Hence, accurate and fast following of the reference opening angle by the electronic throttle has direct economical and ecological impacts.

The synthesis of a satisfactory ETC system is difficult due to the presence of two strong nonlinear effects in the throttle: friction in the gearbox and so-called limp-home (LH) nonlinearity (i.e., the stress-strain characteristics of the return spring) [3]. Moreover, the controller should be implementable on a simple microcontroller, while it has to be robust for a range of process parameters variations (caused either by the parameter deviations in production, change of the working conditions, or by the component aging). Additionally, the control strategy should respect physical limitations of the throttle control input and safety constraints on the process variables (e.g., dc motor current) prescribed by the manufacturer [4].

Considering everything mentioned before, it is not a surprise that this challenging automotive control problem has attracted significant attention of the research community and automotive industry in the last decade. Most of the existing control designs use a linear model of the process and derive a PID [3], [5] or a Linear Quadratic Gaussian (LQG) [6], [7] controller with system nonlinearities compensated by the heuristically tuned compensators. These control systems are simple to implement and if properly tuned, they provide fast transient responses without overshoot, good static accuracy, and robustness to the expected range of the process parameters variations. However, it is not clear how the compensator parameters should be chosen to guarantee stability and/or the prespecified closed-loop performance without extensive tuning. Moreover, for the initial tuning of the controller a detailed identification of the throttle physical parameters is necessary. At the expense of introducing new tuning parameters, the identification requirement can be partially alleviated by using the self-tuning and autotuning methods proposed in [8]. Furthermore, the compensators are usually of a bang-bang type and the limit cycles which they induce in the closed-loop response have to be treated by additional logic or prefilters. This, usually, renders the systematic analysis of the compensator interference with

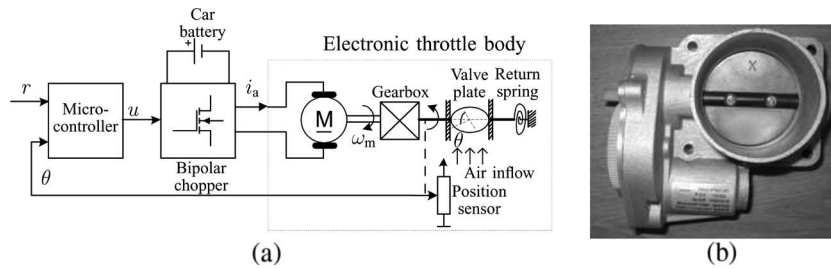


Fig. 1. Electronic throttle. (a) ETC system. (b) ETB.

the linear controller intractable. Last but not least, such control strategies do not systematically take into account constraints on the control input and they cannot guarantee satisfaction of safety constraints for the throttle state variables.

A number of the reported ETC designs utilizes robustness property of the sliding-mode control technique to the system uncertainty [9]–[11]. For example, in [11], a linear model of the throttle is used where the nonlinearities together with the disturbances are treated as uncertainties which are compensated with an online tuned neural network. This approach results in a relatively fast, well-damped, and accurate response of the control system, with a low-level control voltage activity, and excellent robustness to the throttle parameters variations. The control algorithm ensures the boundedness of all signals and neural network parameters. Unfortunately, the control scheme requires high computational power due to the quasi-continuous-time implementation (i.e., a very small sampling time) and is thus inappropriate for the microcontroller implementation. Furthermore, this control strategy does not explicitly take into account the constraints on process variables.

In this paper, the weak points of the existing electronic throttle controller designs are addressed by the use of a model predictive control (MPC) [12] strategy for hybrid systems.¹ This systematic nonlinear model-based controller design procedure takes into account all modeled process nonlinearities and provides the optimal control system performance, while fulfilling all imposed constraints on process variables. In particular, the piecewise affine (PWA) approximations are used to model system nonlinearities. Then, a constrained time-optimal control (CTOC) problem for the PWA process model is formulated that ensures the fastest possible tracking of the reference while respecting all the constraints. The computation of the optimal controller action can be restated as a mixed-integer program [13]. Since the sampling time of the plant is small and a simple microcontroller should be used, online computation of the optimal control input using mixed-integer programming solvers is too prohibitive. To overcome that problem, similarly as in [14], the control law is precomputed offline for the range of model states and references by combining dynamic programming strategy with the reachability analysis for the PWA model. The resulting controller guarantees that for any constant reference the tracking error remains within a small bounded set, while the control law has a (PWA) lookup table form and is therefore easily implementable on low-cost hardware. The

advantage of our controller is that for a fixed model structure its design steps can be practically automated.

This paper is an extension of our recently published work [15] that describes the evolution of the MPC strategy used for the ETC system. In [15], based on the ideas from [14], the time-optimal controller was computed by using multiparametric programming. Here, we employ the controller computation based on reachability analysis that additionally exploits the fact that the electronic throttle is a single-input process. This results in further simplification of the control law [16]. If one considers the memory requirements of today's automotive microcontrollers [2] and compares it with the controller presented in this paper, the obvious conclusion is that the controller design for automotive systems based on hybrid systems theory is no longer only of academic nature.

This paper is organized as follows. In Section II, the electronic throttle and its continuous-time (CT) nonlinear model are described. A discrete-time (DT) PWA model of the throttle, used for the optimal controller synthesis, is derived in Section III. The offline control law computation and its online evaluation procedure for the time-optimal control strategy are presented in Section IV. Finally, the experimental results are reported in Section V.

II. ELECTRONIC THROTTLE

The throttle is a valve used in vehicles to regulate air inflow into the engine combustion system. The air throughput is controlled by the opening angle of the valve plate in the air tube. For a long time, the throttle valve plate was directly connected to the gas pedal by a cable. The reason being that the amount of air inflow is proportional to the desired engine speed, which is decided by the position of the gas pedal. Nowadays, however, the throttle cable is substituted with the throttle-by-wire system. The gas pedal sensor provides the driver command to the ECU which then specifies proper air–fuel mixture to be fed into the engine. In particular, the ECU calculates, based on the complex lookup tables, the references for the fuel injection control system, and for the control system that positions the throttle valve in the desired opening angle—the ETC system. The ETC system with fast and accurate following of the ECU opening angle references results in a better performance and fuel economy compared to the mechanical throttle.

The ETC system [the principal functional scheme given in Fig. 1(a)] comprises a controller (typically implemented in a microcontroller), a bipolar chopper and an electronic throttle. The electronic throttle consists of a dc drive (powered by the

¹Hybrid systems are systems with both discrete- and continuous-valued variables.

chopper), a gearbox, a valve plate, a dual return spring, and a position sensor. All throttle components are assembled in a compact electronic throttle body (ETB), shown in Fig. 1(b), which is mounted on the engine air tube. As depicted in Fig. 1(a), the control signal is fed to the bipolar chopper, which supplies the dc drive with the appropriate armature voltage. The armature current created induces the motor torque that is transmitted through the gearbox to the throttle plate. The valve plate movement stops when the motor torque is counterbalanced by the torque of the dual return spring, the gearbox friction torque, and the load torque induced by the air inflow. The opening angle of the valve corresponds to the angle between the valve plate and the air tube cross section [4], and it spans from 13° (closed valve—no air inflow) to 103° (totally opened valve). At the extreme valve positions, mechanical safety stops prevent further valve plate shaft movement. The opening angle is measured by the potentiometer sensor and this is the only feedback signal available in the standard ETC system.

A. Demands on the ETC System

The engineering practice in automotive industry sets the following demands on the ETC system [3].

- 1) Settling time of the reference step response must be less than 100 ms for any operating point and any reference step change. The steady-state error must be less than 0.1° .
- 2) No overshoot in the reference step response.
- 3) Activity of the control input signal must be low in the steady state.
- 4) The dc motor current must adhere to the limits specified by its vendor.
- 5) The control system should be robust to the variations of the process parameters caused either by production deviations, variations of external conditions, or aging.
- 6) The control strategy must be simple enough to be implementable on the automotive microcontroller system regarding both the processing time and memory requirements. Moreover, the controller synthesis should be simple, transparent, and automated as much as possible.

All control objectives previously mentioned have a clear impact on the performance of the overall system. Fast settling time brings benefits regarding the fuel efficiency and exhaust gas emissions. It also improves the drivability of the car because it makes the superimposed engine torque control system faster. Accurate positioning is especially important for the idle-speed control since it can eliminate the need for the additional actuator whose purpose is to dose the air when the throttle valve is closed. Lower activity of the control signal prevents the excessive wear of the transmission components and position sensor, and reduces the motor losses.

B. CT Model of the Electronic Throttle

In our further discussion, we will consider the assembly of the electronic throttle and the chopper as a plant. Its dynamical

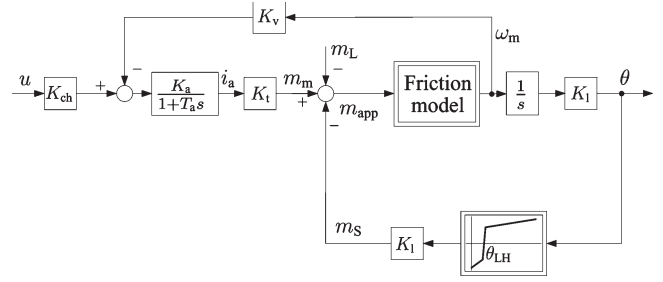


Fig. 2. Nonlinear CT model of the electronic throttle with chopper.

behavior can be described with the following equations:

$$L_a \frac{di_a}{dt} + R_a i_a = K_{ch} u - K_v \omega_m \quad (1)$$

$$m_m = K_t i_a \quad (2)$$

$$m_{app} = m_m - m_S - m_L \quad (3)$$

$$J \frac{d\omega_m}{dt} = m_{app} - m_f \quad (4)$$

$$\frac{d\theta}{dt} = K_l \omega_m \quad (5)$$

$$\frac{dm_f}{dt} = f_f(m_f, \omega_m) \quad (6)$$

$$m_S = m_S(\theta) \quad (7)$$

where u [V] is the input control voltage, K_{ch} is the chopper gain, i_a [A] is the dc motor armature current, m_m [N · m] is the motor torque, m_S [N · m] is the return spring torque, m_L [N · m] is the load (disturbance) torque, m_{app} [N · m] is the so-called applied torque, m_f [N · m] is the friction torque, ω_m [rad/s] is the motor angular velocity, θ [°] is the position (opening angle) of the throttle plate, R_a [Ω] is the overall resistance of the armature circuit, L_a [H] is the overall armature inductance, K_t [N · m/A] is the motor torque constant, K_v [V · s/rad] is the electromotive force constant, K_l is the gear ratio, and J [kg · m²] is the overall moment of inertia referred to the motor side. All listed torques are also referred to the motor side. The full nonlinear model of the plant is shown in Fig. 2.

System sampling time of $T = 5$ ms is chosen with respect to the dominant electromechanical time constant of the linearized electronic throttle model ($T_m = J/(K_a K_v K_t) = 14$ ms, see [3] for more details). Because $T_a = L_a/R_a \approx 0.5$ ms $\ll T$, the armature current dynamics can be neglected and (1) is replaced with

$$i_a = K_a (K_{ch} u - K_v \omega_m) \quad (8)$$

where $K_a = 1/R_a$.

The two major process nonlinearities—friction (6) and LH (7) nonlinearity are discussed next.

1) *Friction Nonlinearity*: Friction acts to suppress the relative movement of two contacting surfaces. In the ETB, friction occurs in the gearbox as well as in the throttle valve and motor shaft bearings. It is an unavoidable phenomenon, especially in a mass production assembly of mechanical transmissions made out of cheap components. It is usually left to the control

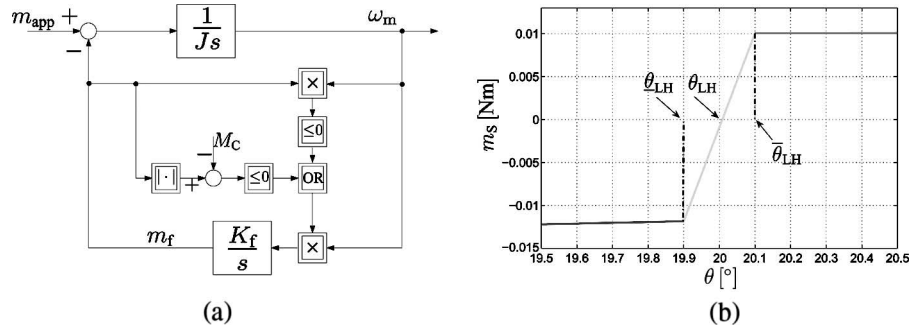


Fig. 3. Nonlinearities in the CT electronic throttle model. (a) CT reset-integrator friction model. (b) Return spring stress–strain characteristics [4]. Detail around θ_{LH} .

algorithm to compensate friction properly and in most cases controller needs information about the friction model.

Probably the easiest way to model the friction effect is to describe it as a simple static characteristic. However, friction in the throttle gearbox is characterized by a significant presliding effect [3] where the valve motion begins well before the applied torque reaches the value of the static friction torque. The presliding motion continues until the full presliding displacement ($\theta_{ps} \approx 0.3^\circ$) is reached at which point the friction torque is equal to the static friction torque. This phenomenon is crucial to model since our tracking system has to be accurate up to the measurement resolution ($\approx 0.1^\circ$). Therefore, the controller must be based on a dynamic friction model. For more details on presliding in the throttle application and the reasons for the use of a dynamic friction model, see [15]. A survey on friction modeling can be found in [17].

Dynamic friction model includes an additional state to model straining of the bonds in the asperity contacts. Since the friction torque is proportional to the straining of the asperity contact bonds, we model this effect with (6). In particular, we use the reset-integrator model [18], [19] which, essentially, describes friction as a switched linear function of the following form [see the block scheme in Fig. 3(a)]:

$$\frac{dm_f}{dt} = \begin{cases} 0, & \text{if } \begin{cases} \omega_m \geq 0 & \text{and } m_f \geq M_C \\ \omega_m \leq 0 & \text{and } m_f \leq -M_C \end{cases} \\ K_f \omega_m, & \text{otherwise} \end{cases} \quad (9)$$

where M_C is the Coulomb friction torque, K_f [$\text{N} \cdot \text{m}/\text{rad}$] is a parameter. The value of parameter K_f ensures that at the end of the presliding movement the friction torque reaches the Coulomb friction torque, i.e.,

$$K_f = \frac{M_C}{\frac{\pi}{180} K_1 \theta_{ps}}. \quad (10)$$

Note that the reset-integrator model (9) is well suited for the derivation of a DT PWA (DTPWA) process model, which is not necessarily the case with other dynamic friction models. For example, the LuGre friction model [20] can accurately describe the presliding effect but it is governed by a nonlinear differential equation that is difficult to linearize.

2) *LH Nonlinearity*: Following manufacturer's specification, in the case of a power failure, the throttle valve has to be placed in the so-called LH position. This position enables the

vehicle to “limp” to the nearest repairing facility since there is some inflow of air to the car engine. The LH position is ensured with the highly nonlinear stress–strain curve of the dual return spring. In this paper, θ_{LH} of about 20.0° is used, which actually corresponds to 7° of the relative opening of the valve plate. The (probably discontinuous) characteristic of the spring in the narrow LH region is interpolated as shown in Fig. 3(b) to get a continuous static characteristic of the nonlinear plant model.

3) *Other Nonmodeled Nonlinear Effects*: The electronic throttle exhibits other (less significant) nonlinear effects which are not modeled here: backlash, change of the armature resistance due to motor commutation (reported in [5]), and measurement quantization.

Gearbox backlash is significant in the LH region where the dual spring may not prestrain the gears and thus a free movement of the gear wheel tooth on the motor side between the two corresponding teeth on the valve shaft side can be expected. However, we neglect this effect since, in our case, the LH region is narrow and due to the measurement quantization only one digital value of the angle can be registered in it. Outside the LH region the gears are definitely prestrained by the return spring. Hence, the backlash may only be observed for fast dc motor stoppings and reversals, which are not crucial for the steady-state accuracy nor they have any significant impact on the transient response of the system.

Laboratory testings in [5] report significant variation of the armature resistance within a single motor rotation due to the commutation effects. However, such effects were not detected in our experimental setup.

The low-quality of the available angle measurement—with 0.11° quantization level—is a serious obstacle when one considers the desired static accuracy of the closed-loop system. In our experiments, the measurement quantization was (adequately) treated with a state estimator/smoothing [21].

III. DTPWA MODEL OF AN ELECTRONIC THROTTLE

The conventional design of a digital control system usually starts with a DT linear plant model. Any additional nonlinearities are treated with heuristically tuned compensators. The common argument that “this works” covers the pitfalls of such a design—an extensive tuning of many controller parameters, with no guarantees for the stability of the closed-loop system. In contrast to that, the MPC concept offers systematic handling of nonlinear plant models. It achieves optimal system performance

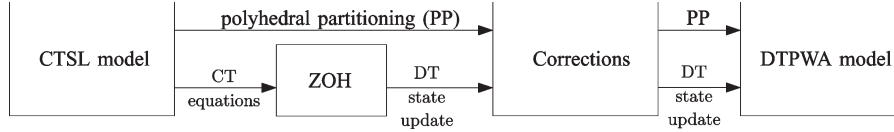


Fig. 4. Derivation of the DTPWA model from the CTSL model of the system.

while guaranteeing the closed-loop stability and ensuring satisfaction of the (prescribed) constraints.

We use the MPC with a DT model that comprises several affine equations each of which describes the system behavior for a separate range of process variables. This so-called DTPWA model belongs to the class of DT linear hybrid models [22]. The state-space description of such models, with affine state-update equations (henceforth referred to as dynamics) defined over polyhedra² in the state + input space, is as follows:

$$\begin{aligned} x_{k+1} &= A_i x_k + B_i u_k + f_i \\ y_k &= C_i x_k \\ \text{if } \begin{bmatrix} x_k \\ u_k \end{bmatrix} &\in \mathcal{D}_i, \quad i = 1, \dots, s \end{aligned} \quad (11)$$

where $x \in \mathbb{R}^n$ is the model state, $y \in \mathbb{R}^p$ is the output, $u \in \mathbb{R}^m$ is the control input, $\{\mathcal{D}_i\}_{i=1}^s$ is a polyhedral partition of the state + input space \mathbb{R}^{n+m} , and k denotes the sampling instant.

A. Model Derivation

A DTPWA throttle model is derived from the CT nonlinear model of the system (given in Section II). As a consequence of our choices of friction and LH nonlinearity models, the overall system is actually described as a CT switched linear (CTSL) model. Thus, there is no need to choose linearization points which would undesirably increase the number of degrees of freedom for the controller design. The procedure of obtaining a DTPWA model from the CTSL model is illustrated in Fig. 4. Because we start with a switched linear CT model, initially the same state-space partitioning is used both in continuous and discrete time. Thus, the first step is to obtain the DT state update equations by discretizing, with zero-order hold (ZOH), all linear dynamics of the CT model.

However, the time discretization may introduce some unwanted behavior in the DT model that does not occur in the CT model. Namely, there is no guarantee that the outputs of the DT and CT systems will not differ at sampling instances (unlike in the case of the CT linear system discretization). This discrepancy is caused by the fixed sampling time of the DTPWA model (11) which implies that the switching between dynamics can happen only at integer multiples of the sampling time (whereas in the CTSL model the switching can happen at any moment). The most critical are those samples when the model switches between substantially different dynamics (e.g., zero-crossing of the angular velocity in the case of a DT friction model) and the effect gets worse as the sampling time grows. Thus, if the sampling time is too large, the state update equation $x_{k+1} = A_i x_k + B_i u_k + f_i$ might “move” the state too deep into the region with a substantially different dynamics.

²Polyhedron is defined as an intersection of a finite number of half-spaces.

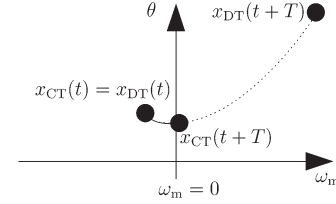


Fig. 5. Illustration of the problematic behavior of the DT model without corrections.

The problem is illustrated (see Fig. 5) with the case of a velocity zero-crossing when modeling friction nonlinearity. Suppose that both the CT and the DT model are in the same state at a time instant $t = kT$, represented with $x_{CT}(t) = x_{DT}(t)$. In Fig. 5, we show projection of those states on the (ω_m, θ) space. Let the applied torque m_{app} be close to zero and let the plant be in sliding friction mode with negative (initial) velocity, i.e., the friction torque $m_f(t) = -M_C$ is trying to accelerate the plate. Suppose that the friction torque is strong enough to stop the plate movement by the next sampling instant. This indeed happens for the CT model, which finds itself in $x_{CT}(t+T)$, but it might not happen in the case of the DT model. Namely, if the zero-velocity is reached at $t + \Delta t$, with $\Delta t < T$, the DT model will continue to use the same dynamics from $t + \Delta t$ to $t + T$ since it cannot switch dynamics between two samples. This would result in the angular velocity rising above zero, i.e., (due to this unnatural behavior) the DT model would reach the faulty state $x_{DT}(t+T)$. Continuing this analysis, one would find long-lasting oscillations of x_{DT} around zero velocity—a behavior that does not happen in practice. Unfortunately, for the throttle application the aforementioned effect cannot be neglected since the sampling time has to be large enough to predict the whole transient response of the system in a small number of steps (otherwise, the optimal control law could become too complex).

The arising effect, which we refer to as the DT switching effect, is resolved by predicting the possible ω_m zero-crossing. The initial PWA model (11) is additionally partitioned along the borders $\omega_{m,i,k+1} = 0$, where $\omega_{m,i,k+1}$ denotes the one-step ahead prediction of ω_m at the discrete instant k using the i th affine dynamics. In the so-called ω_m nonzero-crossing case (i.e., when ω_m and $\omega_{m,i,k+1}$ have the same sign), the i th affine dynamics is used for the state-update. In the ω_m zero-crossing case (i.e., when ω_m and $\omega_{m,i,k+1}$ have the opposite signs), the plate is stuck (stiction) for at least one sample, according to the following “sticking” state-update equations:

$$\omega_{m,k+1} = K_m m_{app,k} \quad (12)$$

$$\theta_{k+1} = \theta_k + \frac{180 K_1 J \omega_{m0}}{\pi M_C} \omega_{m,k} \quad (13)$$

$$m_{f,k+1} = m_{app,k} \quad (14)$$

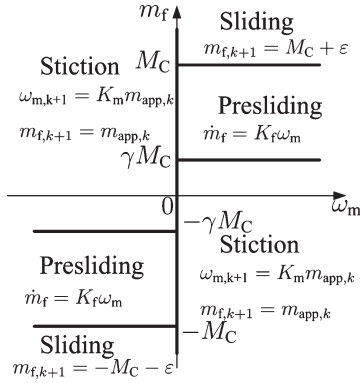


Fig. 6. Borders of affine characteristics regions for the dynamic DTPWA friction model in the (ω_m, m_f) plane (thick lines).

where $K_m = 1$ [rad/N · ms], so that the torques around 0.005 N · m observed in practice produce a very small speed for stiction. The value $\omega_{m0} = 8$ rad/s in (13) is chosen as the statistical mean value of motor angular velocities for which the valve can be stopped due to friction in one sampling instant with $m_{app} = 0$ —the maximal angular velocity that can be stopped by friction within $T = 5$ ms is $M_C T / J = 25$ rad/s. Namely, if the change of the applied torque due to electromotive force and change of the angle is neglected, for the change of the angle θ when entering stiction from sliding the following holds:

$$\Delta\theta = \frac{180K_t J}{2\pi(\text{sign}(\omega_m)M_C - m_{app,k})} \omega_{m,k}^2. \quad (15)$$

More tedious calculations could also account for the effect of applied torque in the linearization used in (13).

The sticking state-update equations (12)–(14) effectively enforce ω_m and m_f to always have the same sign, thus ruling out the DT switching effect in the DTPWA model.

In the CT model (9), both stiction and presliding are modeled using the same expression: $\dot{m}_f = K_f \omega_m$. In the DT model, however, we differentiate between the two modes (see Fig. 6). During stiction, m_{app} is so close to zero that there is no movement of the valve plate. In this case, the states are updated according to (12)–(14), again to avoid the DT switching effect, that could potentially be misused by the model-based controller. To enter the presliding and for the movement to start, m_f tied to m_{app} must in absolute value reach γM_C , where γ is a small positive number. Only when the movement starts the dynamics obtained by the ZOH discretization of the linear model (with $\dot{m}_f = K_f \omega_m$) is used for the state-update. Note also that the model allows for the applied torque pulse which can force the model to skip the presliding altogether and enter the sliding directly from stiction. In sliding, where $\dot{m}_f = 0$, we use a small positive number ε to increase the absolute value of variable m_f over the value M_C in the state-update. Thus, we avoid the situation where the model is on the border of sliding and presliding at the next sampling instant. The model stays in sliding until the velocity zero-crossing is detected. The borders of the friction model in the (ω_m, m_f) plane are depicted in Fig. 6. Note that the borders introduced by one-step-ahead prediction of ω_m are not depicted in Fig. 6, since they involve all the states and inputs and cannot be displayed in

2-D. Note also that this additional partitioning happens only in the presliding and sliding dynamics, i.e., when the valve plate moves. In conclusion, for the regions where stiction or velocity zero-crossing occurs, either in sliding or presliding, the sticking state-update is used. Elsewhere, the state-updates stemming from the ZOH discretization of corresponding linear dynamics in the CTSL model are used. The final DT friction model consists of ten affine dynamics: six depicted in Fig. 6 and four additional arising from the ω_m zero-crossing detection in each sliding and presliding region.

B. Model Complexity

The state and output vectors of the DTPWA model (11), with $m = 1, n = 3, p = 1$, are defined as

$$\begin{aligned} x &= [\omega_m \quad \theta \quad m_f]^T \\ y &= \theta. \end{aligned} \quad (16)$$

The DTPWA model of the electronic throttle is constructed by combining each of ten affine dynamics of friction with each of three affine segments of the LH nonlinearity, thus giving 30 affine dynamics in total. Due to the numerical reasons connected with the controller computation, internal friction torque state m_f is scaled to fall within the order of magnitude of 100, like other two state variables.

C. State Estimation

The valve plate angle θ is the only DTPWA model state measurable on the real ETB. It is measured by a dual potentiometer attached to an A/D converter, with the quantization level of 0.11° . Since the MPC is a full-state feedback strategy, the nonmeasured states ω_m and m_f have to be estimated. The model used in the estimator is

$$x_{k+1} = F(x_k, u_k, v_k) \quad (17)$$

$$z_k = H(x_k, w_k) \quad (18)$$

where $v \in \mathbb{R}^{n_v}$ is the process noise, $z \in \mathbb{R}^p$ the system output burdened with the measurement noise $w \in \mathbb{R}^{n_w}$, $F: \mathbb{R}^{n+m+n_v} \rightarrow \mathbb{R}^n$ and $H: \mathbb{R}^{n+n_w} \rightarrow \mathbb{R}^p$ are nonlinear functions. It is assumed that the state and noise distributions can be approximated with Gaussian random variables which are completely determined with their expectation and covariance. In our case, F is PWA and H is a linear function, v corresponds to the load torque m_L [see (3)] and w is the additive A/D conversion quantization noise. For more details on the electronic throttle state estimation we refer the reader to [21] where the use of the two most common nonlinear model state estimators—extended Kalman filter and unscented Kalman filter (UKF) [23]—is described. In this paper, the UKF is utilized for the purpose of the online state estimation.

IV. TIME-OPTIMAL ELECTRONIC THROTTLE REFERENCE TRACKING

The optimal controller design considered in this paper is based on the process model, the prespecified optimization

criterion and the constraints that the process variables must satisfy on a prediction horizon [12]. The model is used for the prediction of the state trajectory over the horizon based on the current state and the sequence of planned control actions. According to the receding horizon control principle, only the first control input in the optimal control sequence³ (referred to as the optimal control input) is applied to the process, and the whole procedure is repeated at the next sampling instant for the new state measurement. The optimal control input can be obtained either by performing constrained optimization online or by a simple evaluation of a precomputed (offline) state-feedback control law.

If the model is DTPWA, constrained optimal control problem can be restated as a (computationally expensive) mixed-integer program. On the other hand, for the most common optimization criteria and for linear constraints the offline computed explicit control law has a very simple lookup table form [24]. Since the computation time needed for acquiring the optimal control input must be negligible compared to the process sampling time, the online optimizations are possible only for simple and slow models. Since the DTPWA electronic throttle model fits in neither of these two categories, and since the optimal controller is aimed to be implemented on a simple microcontroller, the optimal control law for the throttle must be precomputed offline.

Before formulating the optimal electronic throttle reference tracking problem, which will be solved offline, we first extend the DTPWA model and explicitly enumerate constraints on the throttle variables.

A. Extended System and Constraints

The optimal reference tracking problem for the electronic throttle is formulated in the augmented state + input space

$$\bar{x}_k = \begin{bmatrix} x_k \\ u_{k-1} \\ r_k \end{bmatrix} \quad (19)$$

$$\bar{u}_k = u_k - u_{k-1} \quad (20)$$

where $r_k \in \mathbb{R}^p$ denotes the reference that the system output y_k should follow and \bar{u}_k is the change of the controller action (which is, conveniently, equal to zero at steady-state for any value of the reference). The augmented state-space is $\bar{\mathcal{X}} \subset \mathbb{R}^5$ and the set of inputs to the augmented system is denoted with $\bar{\mathcal{U}} \subset \mathbb{R}^1$. The output \bar{y}_k of such an augmented system is the tracking error itself

$$\bar{y}_k = r_k - y_k. \quad (21)$$

The augmented PWA system is constructed from (11) by using (19)–(21), and the fact that r is kept constant along the prediction horizon, i.e., $r_{k+1} = r_k$

$$\bar{x}_{k+1} = \bar{A}_i \bar{x}_k + \bar{B}_i \bar{u}_k + \bar{f}_i \quad (22a)$$

$$\bar{y}_k = \bar{C}_i \bar{x}_k \quad (22b)$$

$$\text{if } [\bar{x}_k^T \quad \bar{u}_k^T]^T \in \bar{\mathcal{D}}_i, \quad i = 1, \dots, s. \quad (22c)$$

³Any control sequence that satisfies the constraints and achieves the optimal value of the optimization criterion is called the optimal control sequence.

In the rest of this paper, (22a)–(22c) are denoted in a shorter form

$$\bar{x}_{k+1} = \bar{f}_{\text{PWA}}(\bar{x}_k, \bar{u}_k). \quad (23)$$

Furthermore, without loss of generality, it is assumed that polyhedra $\bar{\mathcal{D}}_i$, $i = 1, \dots, s$ already incorporate all the constraints on the states and input, either existing as physical process constraints or being introduced to protect the throttle components from the excessive wear

$$C^x \bar{x}_k + C^u \bar{u}_k \leq C^c. \quad (24)$$

The set of feasible augmented states extracted from (24), denoted with $\mathcal{P} = \{\bar{x} | \mathcal{P}^x \bar{x} \leq P^c\}$, can be computed as

$$\mathcal{P} = \{\bar{x} | \exists \bar{u} : C^x \bar{x} + C^u \bar{u} \leq C^c\} \quad (25)$$

where C^x , C^u , C^c , P^x , and P^c are matrices of appropriate dimensions.

In our experimental setup, physically possible throttle angles are in the range from 12.8° to 103.4°. Since the valve plate must not hit the mechanical stops, posed constraints on the angle are the same as the physical ones. The same constraints are used for the reference r_k . The angular velocity on the motor side ω_m is constrained between $-\omega_{m,\text{lim}}$ and $\omega_{m,\text{lim}}$, where $\omega_{m,\text{lim}} = 150$ rad/s. These constraints, together with the armature current constraints of $\pm i_{a,\text{lim}} = \pm 2$ A, are introduced to extend the working life of the throttle. The input signal u_k is physically limited to ± 5 V, due to the D/A-card and chopper characteristics. The same constraint is used for \bar{u} to forbid the excessive control signal chattering.

B. Offline Computation

In [15], we discussed two optimal control problems formulations for the electronic throttle—the constrained finite time optimal control (CFTOC) and the CTOC. Both strategies ensure that the constraints on the variables are fulfilled during the transient. In the CFTOC problem, the criterion to be minimized is formulated as a sum of norms on the states and inputs over the prediction horizon. It was solved offline for the electronic throttle regulator case, but the extension to the reference tracking case was not possible since the resulting lookup table was too complex to be computed and implemented. On the other hand, for a given state, the CTOC strategy looks for any control sequence that steers the state into a predefined set in the state-space in minimum-time. This predefined set usually has the control invariance property [25], i.e., for any state from the set there exists a feasible control action (that is the one that does not violate the constraints) that keeps the state at the next time instant in the same set. Thus, the CTOC synthesis consists of two parts: 1) finding an invariant set together with a control law on it that guarantees the set invariance property and, once it is found, 2) finding the appropriate control law for all the process states outside the invariant set such that the state is steered into the invariant set in minimum-time (time-optimal). The CTOC problem formulation results in much simpler control laws compared to CFTOC (cf., [15] and [26]).

The procedure used for the CTOC synthesis in [15] strictly followed the ideas from [26], where the invariant set is created iteratively for a prefixed control law [27] and the state space outside the invariant set is explored using dynamic programming strategy that incorporates multiparametric quadratic programming and geometric manipulations of polytopes [24]. The major modification in [15] compared to [26] is the reduction of the number of switches between the DTPWA model dynamics along the predicted time-optimal transient. The procedure in [15] results in an implementable, albeit storage-wise very demanding, control law. Because of that, the range of the states for which the optimal control law can be constructed is rather limited.

Here, we propose a different procedure, both for an invariant set computation and for the controller construction outside such a set. The modifications reside on a reachability analysis for PWA systems and they are mainly possible due to the fact that the electronic throttle has only one control input. The procedure does not need multiparametric programming solvers. This results in a significant shortening of the offline computation time, reduction of controller complexity—especially concerning the memory demands, and shortening of the online control law evaluation time. All of these three issues are critical for the MPC application.

1) *Invariant Set Computation:* A control invariant set

$$\mathcal{X}^I = \{\bar{x} | \exists \bar{u} : \bar{f}_{\text{PWA}}(\bar{x}, \bar{u}) \in \mathcal{X}^I\} \quad (26)$$

is computed in an interior of the so-called tracking origin \mathcal{T}^0 —a small predefined polytopic subset of the set of feasible augmented states \mathcal{P} . In this paper, the tracking origin is defined around the intersection of the hyperplanes $r = y$ and $\omega_m = 0$

$$\mathcal{T}^0 = \{\bar{x} \in \mathcal{P} | |\omega_m| < 1, |r - \theta| < 0.1\}. \quad (27)$$

The invariant set \mathcal{X}^I is, in general, computed in an iterative manner. At the iteration step q (starting with $q = 0$) a set $\mathcal{H}_i^{0,q} \subset \bar{\mathcal{X}} \times \bar{\mathcal{U}}$, $i = 1, \dots, s$, is computed for which the augmented system state \bar{x} can enter \mathcal{T}^q in one time instant using dynamics i while respecting all constraints defined by the polyhedron $\bar{\mathcal{D}}_i$

$$\mathcal{H}_i^{0,q} = \{[\bar{x}^T \ \bar{u}^T]^T \in \bar{\mathcal{D}}_i | \bar{A}_i \bar{x} + \bar{B}_i \bar{u} + \bar{f}_i \in \mathcal{T}^q\}. \quad (28)$$

A target set for the next iteration step is then computed as

$$\mathcal{T}^{q+1} = \mathcal{T}^q \cap \left(\bigcup_{i=1}^s \mathcal{R}_i^{0,q} \right) \quad (29)$$

where $\mathcal{R}_i^{0,q}$ denotes the projection of $\mathcal{H}_i^{0,q}$ on the $\bar{\mathcal{X}}$ space, i.e.,

$$\mathcal{R}_i^{0,q} = \left\{ \bar{x} \in \bar{\mathcal{X}} | \exists \bar{u} \in \bar{\mathcal{U}} : [\bar{x}^T \ \bar{u}^T]^T \in \mathcal{H}_i^{0,q} \right\}. \quad (30)$$

Remark 1: In the throttle application, \bar{u} is 1-D, i.e., $\bar{\mathcal{U}} \subset \mathbb{R}$. Assume that \mathcal{T}^q is a polytope. Let $\mathcal{H}_i \subset \bar{\mathcal{X}} \times \bar{\mathcal{U}}$ be a full-dimensional polyhedron defined by (28) and let \mathcal{R}_i be its projection on $\bar{\mathcal{X}}$. Then, for a given $\bar{x} \in \mathcal{R}_i$, there exists a unique 1-D interval $\mathcal{I}_i(\bar{x}) := [a(\bar{x}), b(\bar{x})] \subset \mathbb{R}$, with $a(\bar{x}) \leq b(\bar{x})$, such that for any $\bar{u} \in \mathcal{I}_i$ the state \bar{x} moves in \mathcal{T}^q at the next time step,

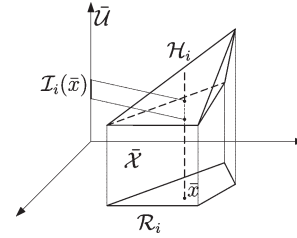


Fig. 7. Determining the interval $\mathcal{I}_i(\bar{x})$.

by using the i th dynamics, while respecting the constraints. For a given \bar{x} , the interval \mathcal{I}_i can be easily computed from the matrix description of \mathcal{H}_i , see Fig. 7 for illustration. If \mathcal{T}^q is given as a nonconvex union of polytopes, then, in general, \mathcal{H}_i also has the form of a nonconvex union of polyhedra. In such a case, feasible control actions \bar{u} might comprise several nonconnected 1-D intervals.

If $\mathcal{T}^{q+1} = \mathcal{T}^q$ the algorithm has finished and the control invariant set is found, with $\mathcal{X}^I = \mathcal{T}^q$. Otherwise, the whole procedure is repeated for the iteration step $q + 1$.

Suppose that the algorithm terminates at iteration q_0 , i.e., $\mathcal{T}^{q_0} = \mathcal{T}^{q_0+1} = \mathcal{X}^I$. For simplicity, in the rest of this paper, the part of the set \mathcal{H}_i^{0,q_0} over \mathcal{T}^{q_0} is denoted with \mathcal{H}_i^0 . Note that this set, as well as its projection \mathcal{R}_i^0 , may be nonconvex for $q_0 \geq 1$, and therefore they are in general represented as unions of polyhedra

$$\mathcal{H}_i^0 = \bigcup_{j=1}^{h_i} \mathcal{H}_{i,j}^0 \quad (31)$$

$$\mathcal{R}_i^0 = \bigcup_{j=1}^{r_i} \mathcal{R}_{i,j}^0. \quad (32)$$

The invariant set \mathcal{X}^I is, thus,

$$\mathcal{X}^I = \bigcup_{i=1}^s \mathcal{R}_i^0 = \bigcup_{i=1}^s \bigcup_{j=1}^{r_i} \mathcal{R}_{i,j}^0. \quad (33)$$

Remark 2: The control law implicitly given by \mathcal{H}_i^0 guarantees only the invariance property of the set \mathcal{X}^I , i.e., the tracking error \bar{y} will be bounded in a small set for constant references. The described procedure does not guarantee that \bar{y} converges to zero. Therefore, in general, limit cycles and/or nonzero equilibrium points might occur. In the special case of a single-output system with the same output matrix for all dynamics ($\bar{C}_i \equiv \bar{C}$, $\forall i$), one can achieve asymptotic convergence of \bar{y} to zero by replacing (28) with

$$\mathcal{H}_i^{0,q} = \{[\bar{x}^T \ \bar{u}^T]^T \in \bar{\mathcal{D}}_i | \bar{A}_i \bar{x} + \bar{B}_i \bar{u} + \bar{f}_i \in \mathcal{T}^q, |\bar{C}(\bar{A}_i \bar{x} + \bar{B}_i \bar{u} + \bar{f}_i)| \leq \delta |\bar{C} \bar{x}|\} \quad (34)$$

where $0 < \delta < 1$ is an upper bound on the asymptotic convergence rate. However, since in our case, the set $\mathcal{X}^I \subseteq \mathcal{T}^0$ falls within the desired positioning accuracy band around the reference, we skip such a computation.

For the online implementation, only the polyhedra that define \mathcal{H}_i^0 , $i = 1, \dots, s$, are needed since from them the interval of feasible control actions (and one specific value of the controller action) can be easily computed. On the other hand, for the further offline construction of the time-optimal control law outside the invariant set only the polyhedra that define \mathcal{R}_i^0 , $i = 1, \dots, s$, are needed.

2) *Time-Optimal Control Law Computation*: The time-optimal control problem for all $\bar{x}_0 \notin \mathcal{X}^I$ is posed as follows:

$$J^*(\bar{x}_0) = \min_{U_k, k} k$$

$$\text{subj. to } \begin{cases} \bar{x}_{k'} = \bar{f}_{\text{PWA}}(\bar{x}_{k'-1}, \bar{u}_{k'-1}) \\ \bar{x}_{k'} \in \mathcal{P} \\ k' = 1, \dots, k \\ \bar{x}_k \in \mathcal{X}^I \end{cases} \quad (35)$$

where $U_k = \{\bar{u}_0, \dots, \bar{u}_{k-1}\}$. The optimal cost corresponds to the minimal number of time steps in which the state \bar{x}_0 can be moved in the invariant set while respecting all constraints. The z th cost-to-go set, denoted with \mathcal{X}^z , $z \in \{1, 2, \dots\}$, is the set of all \bar{x} for which the cost J^* equals z . By definition $\mathcal{X}^0 := \mathcal{X}^I$.

In [26], the solution to (35) is constructed by solving multiparametric programs in a dynamic programming procedure. We also employ the dynamic programming approach when solving (35) but, in contrast to solving the multiparametric programs, here a sequence of one-step reachability computations is carried out. The procedure starts with $z = 1$ and, similarly to the idea in Section IV-B1, computes the set \mathcal{X}^z from \mathcal{X}^{z-1} [recall that $\mathcal{X}^0 := \mathcal{X}^I$, where \mathcal{X}^I is given by (33)] as follows:

$$\mathcal{X}^z = \bigcup_{i=1}^s \mathcal{R}_i^z \quad (36)$$

where \mathcal{R}_i^z is the projection of the set

$$\mathcal{H}_i^z = \{[\bar{x}^T \ \bar{u}^T]^T \in \bar{\mathcal{D}}_i | \bar{A}_i \bar{x} + \bar{B}_i \bar{u} + \bar{f}_i \in \mathcal{X}^{z-1}\} \quad (37)$$

on the $\bar{\mathcal{X}}$ -space.

Note that \mathcal{H}_i^z and \mathcal{R}_i^z are unions of a finite number of polyhedra. The algorithm implementation also (straightforwardly) utilizes the idea from [15] to reduce the switchings between different DTPWA model dynamics while preserving the time-optimality. The switching reduction is important for the avoidance of the DT switching effect described in Section III-A. Moreover, the switching between dynamics is usually connected with a more active control input.

The offline computation stops at iteration $z_m + 1$ if $\mathcal{X}^{z_m+1} = \emptyset$. The maximal controllable set $\mathcal{K}_{\text{PWA}}^\infty \subseteq \bar{\mathcal{X}}$ (for more details see [27]) can then be computed as

$$\mathcal{K}_{\text{PWA}}^\infty = \bigcup_{0 \leq z \leq z_m} \mathcal{X}^z. \quad (38)$$

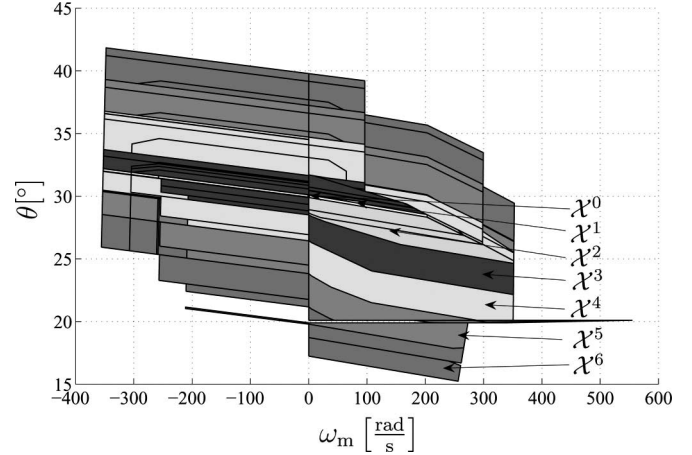


Fig. 8. Invariant set and the first six cost-to-go sets for the electronic throttle with $[m_f \ u_{k-1} \ r] = [60 \ 2 \ 30]$.

In Fig. 8, a cut through the invariant set and first six cost-to-go sets is shown for the electronic throttle application.

C. Online Computation

Online computation of the control action is very simple. For a given \bar{x} , one has to carry out s trivial polytope membership tests to find the set of active dynamics

$$\mathcal{A}(\bar{x}) = \{i | 1 \leq i \leq s, \bar{x} \in \bar{\mathcal{P}}_i\} \quad (39)$$

where $\bar{\mathcal{P}}_i$ denotes the projection of $\bar{\mathcal{D}}_i$ on the $\bar{\mathcal{X}}$ space. Then, a search is performed, starting from \mathcal{X}^0 toward the higher cost-to-go sets, for the first polyhedron in the set \mathcal{H}_i^z , $i \in \mathcal{A}$, that gives a nonempty interval of feasible control actions \bar{u} . Finally, the control action \bar{u} is set to the middle value of the found interval. Thus, the online implementation requires only the elementary controller code and the storage of the sets $\bar{\mathcal{P}}_i$ and \mathcal{H}_i^z . The online control algorithm is noniterative and it consists of elementary algebraic manipulations: multiplications, additions, and comparisons.

Remark 3: Note that for a measured x (i.e., for the induced \bar{x}) one does not have to pass through all polytopes \mathcal{H}_i^z , but only through those with an index $i \in \mathcal{A}$. Since for the electronic throttle, DTPWA model no more than two dynamics out of 30 can be simultaneously active, if we assume that the regions \mathcal{H}_i^z are uniformly distributed over the dynamics then, in the worst case, only 1/15 of all the regions has to be checked to find the time-optimal control action for a given \bar{x} .

V. EXPERIMENTAL RESULTS

The time-optimal control strategy described in Section IV combined with the UKF state estimation is tested on a real electronic throttle—Visteon 3M4U-9F991-AC [4]. The online control scheme with the 2.4-GHz control computer system running Real-Time Linux is depicted in Fig. 9. Even though the armature current measurement is available in our experimental setup, we do not use it in the closed-loop control, since this

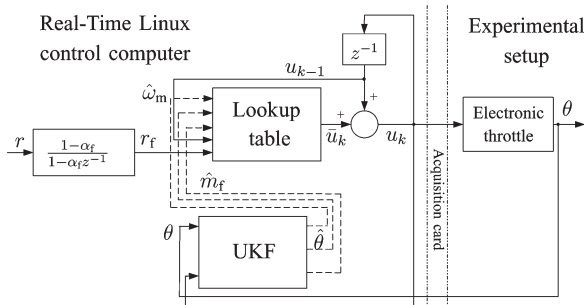


Fig. 9. Online control scheme.

measurement is unavailable in the standard vehicle implementations. A prefilter with 15-ms time constant ($\alpha_f = 0.7165$) is introduced in the reference path to eliminate overshoots in the angle responses and to reduce the number of cost-to-go sets around the invariant set needed for the online computation. Namely, first six cost-to-go sets around the invariant set are used. Without the prefilter, in the case of an abrupt reference change, the extended state could fall outside the space covered with those six cost-to-go sets. The step response settling time of the prefilter is less than 50 ms and its use is thus justifiable since, according to the demand 1 from Section II-A, the ETC system settling time may not go beyond 100 ms. The offline control law computation described in Section IV-B is carried out within Matlab, with the Multi-Parametric Toolbox [28] and NAG linear programming solver [29]. The controller consists of 9221 polyhedral regions $\mathcal{H}_{i,k}^z$ in \mathbb{R}^6 , that are described in their minimal representation with 14 624 different hyperplanes. For the storage of such a controller structure around 970 kB of RAM are needed. The offline computations lasted for about 72 h on a 2.4-GHz Win2k machine.

Both the control and estimation algorithms run with $T = 5$ ms sampling time. In Fig. 10(a), we first show the ETC system response to the 2° square reference under LH zone. The settling time is approximately 50 ms, with a very small overshoot. It can be observed that the control voltage ringing is extremely low (approximately 4 mV) in steady-state, which is very beneficial for the long-lasting component life. This is achieved thanks to the UKF that filters out the measurement noise and outliers (see the measurement at about 31.2 s and its effect to the control voltage). A tuned PID controller with feedforward nonlinearities compensation from [3] resulted in 80 ms transient with 0.25-V steady-state control voltage activity. Similar response properties, although with somewhat shorter settling time, were obtained with the neural network-based sliding mode controller from [11]. In the next Fig. 10(b), a 1° step reference change through the LH zone is reported, where both friction and LH nonlinearity are emphasized. Again, the settling time is about 50 ms, without an overshoot, and it can be justifiably stated that the nonlinearities are compensated. In Fig. 11(a), we show the ETC system response to an 0.2° step reference change under LH zone. As already mentioned, for the idle speed engine control it is crucial to have fast and accurate reference following, even for the small reference angle changes. The figure reveals the settling time of about 40 ms, without an overshoot. Fig. 11(b) shows the control

system response to the ramp reference through LH zone, with a sudden slope change. Very good tracking can be observed, with the tracking error being less than 0.1° everywhere except at the upper boundary of the LH zone, where the valve seems to be stuck until the tracking error builds up to 0.25° . The control voltage activity is significant—approximately 2 V compared to 0.6 V obtained for the ramp reference with a PID controller from [3]. Namely, the controller abruptly reacts once the system leaves the invariant set. This voltage activity could be lowered if the offline computation is performed with a larger tracking origin set \mathcal{T}^0 . Fig. 12(a) shows the 2° stairs reference tracking above LH zone. The responses are nicely damped, with the settling time of about 40 ms. One may note that the controller respects the armature current limit during the transient. In Fig. 12(b), the control system responses to large reference steps of 15° both under and above the LH zone are presented. The settling time is about 65 ms. The increase of the settling time is a consequence of the constraint on ω_m , since one may notice that the controller does not let $|\omega_m|$ to rise above $\omega_{m,\text{lim}}$.

During all of the experiments, the overall computation time within a sample was measured. On our testing equipment, it never exceeded 0.4 ms.

VI. CONCLUSION AND FUTURE WORK

A strong friction effect, nonlinear return spring characteristics and high demands on the overall vehicle performance make the control of an electronic throttle a challenging task. In this paper, an MPC strategy is derived for the electronic throttle that guarantees: 1) time-optimal reference tracking thus improving the fuel economy and reducing the exhaust gas emissions and 2) satisfaction of all constraints imposed on the process states and inputs thus extending the working life of components. The electronic throttle is modeled as a DTPWA system. To that end, a DT friction model based on the CT reset-integrator friction model is derived. It can capture presliding effect and is suitable for the MPC strategy. An offline algorithm is described that computes the optimal control law for the range of the system states and references. The algorithm exploits recently reported results in time-optimal control of hybrid systems.

The optimal controller action for the single-input system can be easily computed online on a low-cost hardware from the implicitly given time-optimal control law (precomputed polyhedra in the state-input space). UKF is used for the estimation of unmeasured PWA model states. Experimental results on a real electronic throttle are reported and compared with the performance of a tuned PID controller that comprises a feedforward compensation of the process nonlinearities. The time-optimal controller achieves considerably faster transient, while preserving the other important performance measures, like the absence of an overshoot and static accuracy within the measurement resolution.

Our future work will include estimation of the load torque m_L to allow the MPC to compensate it. Similar to the approach in [11], any process-model mismatch could then be treated through the compensation of the load torque, by considering such a mismatch as a disturbance in the load torque. Furthermore, we will look into the possibility of merging the proposed

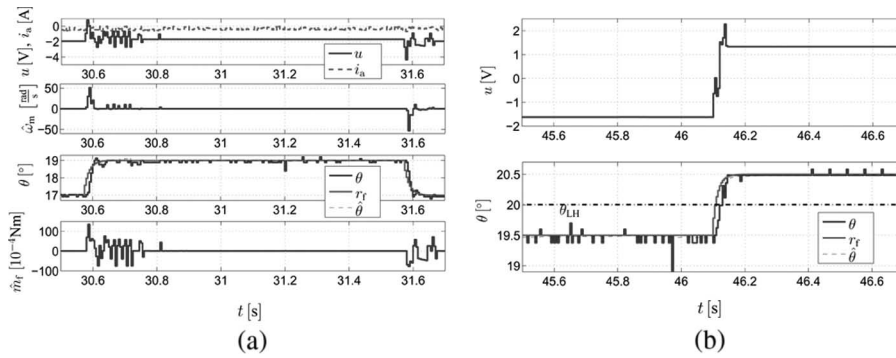


Fig. 10. ETC system responses. (a) Square reference change of 2° under the LH zone. (b) Step reference change of 1° through the LH zone.

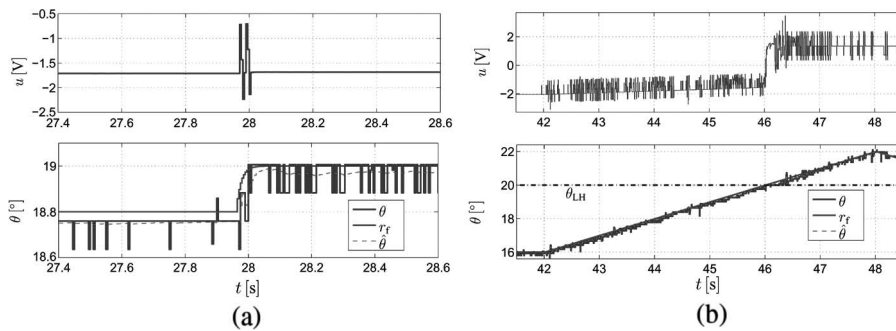


Fig. 11. ETC system responses. (a) Response to the 0.2° step reference change. (b) Response to the ramp reference through the LH zone.

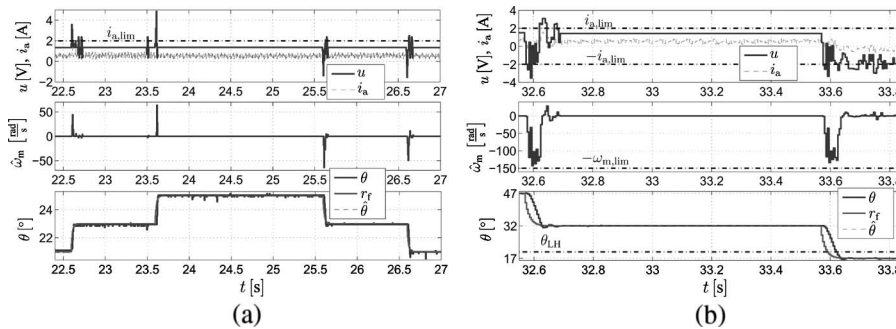


Fig. 12. ETC system responses. (a) Response to the 2° stairs reference above LH. (b) Response to the 15° stairs reference.

controller design procedure with the algorithm for identification of the DTPWA models of nonlinear processes presented in [30]. Such a combination would allow for a practically automated design of the overall ETC system.

ACKNOWLEDGMENT

The author would like to thank D. Pavković for sharing his knowledge about the throttle, M. Barić for help with the Real-Time Linux, and D. Hrovat and J. Deur for helpful discussions regarding the experimental results.

REFERENCES

[1] U. Kiencke and L. Nielsen, *Automotive Control Systems*. Berlin, Germany: Springer-Verlag, 2005.
 [2] J. Lipman, "Silicon fuels the automotive industry," *TechOnLine Publication*, Mar. 2004. [Online]. Available: <http://www.techonline.com>
 [3] J. Deur, D. Pavković, N. Perić, M. Jansz, and D. Hrovat, "An electronic throttle control strategy including compensation of friction and limp-home effects," *IEEE Trans. Ind. Appl.*, vol. 40, no. 3, pp. 821–834, May/June. 2004.

[4] Visteon Corp., *Electronic Throttle Body*, 2006. [Online]. Available: [http://www.visteon.com/products/automotive/throttle body ele.shtml](http://www.visteon.com/products/automotive/throttle%20body%20ele.shtml)
 [5] C. Yang, "Model-based analysis and tuning of electronic throttle controllers," presented at the SAE World Congress, Detroit, MI, 2004, SAE Paper No. 2004-01-0524. [Online]. Available: [http://www.visteon.com/util/whitepapers/2004 01 0524.pdf](http://www.visteon.com/util/whitepapers/2004%2001%200524.pdf)
 [6] J. Gagner and R. Bondesson, "Adaptive realtime control of a nonlinear throttle unit," M.S. thesis, Dept. Autom. Control, Lund Inst. Technol., Lund, Sweden, Nov. 2000. [Online]. Available: <http://www.control.lth.se/documents/2000/5638.pdf>
 [7] A. Kitahara, A. Sato, M. Hoshino, N. Kurihara, and S. Shin, "LQG based electronic throttle control with a two degree of freedom structure," in *Proc. 35th IEEE Conf. Decision and Control*, Kobe, Japan, 1996, pp. 1785–1789.
 [8] D. Pavković, J. Deur, M. Jansz, and N. Perić, "Adaptive control of automotive electronic throttle," *Control Eng. Pract.*, vol. 14, no. 2, pp. 121–136, 2006.
 [9] M. Yokoyama, K. Shimizu, and N. Okamoto, "Application of sliding-mode servo controllers to electronic throttle control," in *Proc. 37th IEEE Conf. Decision and Control*, Tampa, FL, 1998, pp. 1541–1545.
 [10] C. Rossi, A. Tilli, and A. Tonielli, "Robust control of a throttle body for drive by wire operation of automotive engines," *IEEE Trans. Control Syst. Technol.*, vol. 8, no. 6, pp. 993–1002, Nov. 2000.
 [11] M. Barić, I. Petrović, and N. Perić, "Neural network-based sliding mode control of electronic throttle," *Eng. Appl. Artif. Intell.*, vol. 18, no. 8, pp. 951–961, 2005.

- [12] D. Q. Mayne, J. B. Rawlings, C. V. Rao, and P. O. M. Scokaert, "Constrained model predictive control: Stability and optimality," *Automatica*, vol. 36, no. 6, pp. 789–814, 2000.
- [13] F. Borrelli, *Constrained Optimal Control of Linear and Hybrid Systems*, ser. Lecture Notes in Control and Information Sciences, vol. 290. Berlin, Germany: Springer-Verlag, 2003.
- [14] F. Borrelli, M. Baotić, A. Bemporad, and M. Morari, "Dynamic programming for constrained optimal control of discrete-time linear hybrid systems," *Automatica*, vol. 41, no. 10, pp. 1709–1721, 2005.
- [15] M. Vašak, M. Baotić, M. Morari, I. Petrović, and N. Perić, "Constrained optimal control of an electronic throttle," *Int. J. Control*, vol. 79, no. 5, pp. 465–478, 2006.
- [16] S. S. Keerthi and E. G. Gilbert, "Computation of minimum-time feedback control laws for discrete-time systems with state-control constraints," *IEEE Trans. Automatic Control*, vol. AC-32, no. 5, pp. 432–435, May 1987.
- [17] H. Olsson, K. J. Åström, C. Canudas de Wit, M. M. Gäfvert, and P. Lischinsky, "Friction models and friction compensation," *Eur. J. Control*, vol. 4, no. 3, pp. 176–195, 1998.
- [18] D. A. Haessig and B. Friedland, "On the modelling and simulation of friction," *Trans. ASME, J. Dyn. Syst. Meas. Control*, vol. 113, no. 3, pp. 354–362, 1991.
- [19] A. Božić, D. Pavković, J. Deur, and N. Perić, "Friction compensation based on reset-integrator friction model," in *Proc. 9th Eur. Conf. Power Electron. and Appl.*, Graz, Austria, 2001, pp. 1154–1159.
- [20] C. Canudas de Witt, H. Olsson, K. J. Åström, and P. Lischinsky, "A new model for control of systems with friction," *IEEE Trans. Autom. Control*, vol. 40, no. 3, pp. 419–425, Mar. 1995.
- [21] M. Vašak, I. Petrović, and N. Perić, "State estimation of an electronic throttle body," in *Proc. IEEE Int. Conf. Ind. Technol.*, Maribor, Slovenia, 2003, pp. 472–477.
- [22] W. Heemels, B. D. Schutter, and A. Bemporad, "Equivalence of hybrid dynamical models," *Automatica*, vol. 37, no. 7, pp. 1085–1091, 2001.
- [23] E. Wan and R. van der Merwe, "The unscented Kalman filter," in *Kalman Filtering and Neural Networks*, S. Haykin, Ed. New York: Wiley, 2001.
- [24] M. Baotić, "Optimal control of piecewise affine systems—A multi-parametric approach," Ph.D. dissertation, Swiss Federal Inst. Technol. (ETH), Zurich, Switzerland, Mar. 2005. [Online]. Available: <http://control.ee.ethz.ch/index.cgi?page=publications>
- [25] F. Blanchini, "Set invariance in control—A survey," *Automatica*, vol. 35, no. 11, pp. 1747–1767, 1999.
- [26] P. Grieder, M. Kvasnica, M. Baotić, and M. Morari, "Stabilizing low complexity feedback control of constrained piecewise affine systems," *Automatica*, vol. 41, no. 10, pp. 1683–1694, 2005.
- [27] S. Raković, P. Grieder, M. Kvasnica, D. Q. Mayne, and M. Morari, "Computation of invariant sets for piecewise affine discrete time systems subject to bounded disturbances," in *Proc. 43rd IEEE Conf. Decision and Control*, Atlantis, Bahamas, 2004, pp. 1418–1423.
- [28] M. Kvasnica, P. Grieder, M. Baotić, and M. Morari, *Multi-Parametric Toolbox (MPT)*, 2003. [Online]. Available: <http://control.ee.ethz.ch/~hybrid/mpt/>
- [29] The Numerical Algorithms Group, Ltd., *The NAG Foundation Toolbox*. Oxford, U.K., 2002. [Online]. Available: <http://www.nag.co.uk>
- [30] M. Vašak, L. Mladenović, and N. Perić, "Clustering-based identification of a piecewise affine electronic throttle model," in *Proc. 31st Annu. Conf. IEEE Ind. Electron. Soc.*, Rayleigh, NC, 2005, pp. 177–182.



Mario Vašak received the B.Sc. degree in electrical engineering from the Faculty of Electrical Engineering and Computing (FER Zagreb), University of Zagreb, Croatia, in 2003, where he is currently working toward the Ph.D. degree in the Department of Control and Computer Engineering.

His main research interests are robust optimal control and identification of hybrid systems, application of estimation techniques in mechatronics, and computational geometry.



Mato Baotić (S'97–M'01) received the B.Sc. and M.Sc. degrees in electrical engineering from the Faculty of Electrical Engineering and Computing (FER Zagreb), University of Zagreb, Zagreb, Croatia, in 1997 and 2000, respectively, and the Ph.D. degree from Swiss Federal Institute of Technology (ETH) Zurich, Zurich, Switzerland, in 2005.

He is currently a Post-Doctoral Researcher in the Department of Control and Computer Engineering, FER Zagreb, Croatia. He received the Eidgenössische Stipendienkommission für ausländische Studierende scholarship of the Swiss Government for the academic year 2000/2001, which he spent as a Visiting Researcher at the Automatic Control Laboratory, ETH Zurich. His research interests include mathematical programming, hybrid systems, optimal control, and model predictive control.



Ivan Petrović (M'97) received the B.Sc., M.Sc., and Ph.D. degrees in electrical engineering from the Faculty of Electrical Engineering and Computing (FER Zagreb), University of Zagreb, Zagreb, Croatia, in 1983, 1989, and 1998, respectively.

He was an R&D Engineer with the Institute of Electrical Engineering of the Končar Corporation in Zagreb from 1985 to 1994. Since 1994, he has been with FER Zagreb, where he is currently an Associate Professor with the Department of Control and Computer Engineering. He teaches a number of undergraduate and graduate courses in the field of control systems and mobile robotics. His research interests include various advanced control strategies and their applications to control of complex systems, and mobile robots navigation. Results of his research have been implemented in several industrial products.

Prof. Petrović is a member of the International Federation of Automatic Control—Technical Committee on Robotics and Federation of International Robot-soccer Association—Executive Committee. He is a collaborating member of the Croatian Academy of Engineering.



Nedjeljko Perić (M'94–SM'04) received the B.Sc., M.Sc., and Ph.D. degrees in electrical engineering from the Faculty of Electrical Engineering and Computing (FER Zagreb), University of Zagreb, Zagreb, Croatia, in 1973, 1980, and 1989, respectively.

From 1973 to 1993, he was with the Institute of Electrical Engineering of the Končar Corporation, Zagreb, as an R&D Engineer, Head of the Positioning Systems Department, and Manager of the Automation Section. In 1993, he joined the Department of Control and Computer Engineering at FER Zagreb as an Associate Professor. He was appointed as a Full Professor in 1997 and he currently teaches several courses on automatic control. His current research interests are in the fields of process identification and advanced control techniques.

Prof. Perić serves as the Chairman of KoREMA, the Croatian Society for Communications, Computing, Electronics, Measurements and Control. He is also a member of several international professional associations. He is a member of the Board of Editors of the Croatian journal *Automatika*. He is a Fellow of the Croatian Academy of Engineering.